ChemPubSoc Europe

DOI: 10.1002/chem.201405222

CHEMISTRY
A European Journal
Full Paper

Drug Delivery |*Hot Paper*|

A Free-Blockage Controlled Release System Based on the Hydrophobic/Hydrophilic Conversion of Mesoporous Silica Nanopores

Wenqian Wang,[a] Linfeng Chen,[b] Li-ping Xu,[a] Hongwu Du,[a] Yongqiang Wen,*[a] Yanlin Song,[b] and Xueji Zhang*[a]

Abstract: A pH-responsive free-blockage release system was achieved through controlling the hydrophobic/hydrophilic conversion of mesoporous silica nanopores. This system further presented pulsatile release with changing pH values between 4.0 and 7.0 for several cycles. This free-blockage release system could also release antitumor agents to induce cell death after infecting tumor cells and could have the ability of continuous infection to tumor cells with high drug-delivery efficiency and few side effects.

Introduction

The hydrophobic phenomenon exists widely in nature.[1] It is responsible for numerous chemical and biological aspects of molecular interactions in water, such as the water channels through biological membranes, which are employed to control the water and ionic fluxes by the conversion of channels between hydrophobicity and hydrophilicity.[2] With inspiration taken from these natural channels, a series of nanopores has been built with hydrophobic/hydrophilic conversion based on responses to pH value, voltage, light, and bioanalytes.[3]

In recent years, controlled release systems based on mesoporous silica nanoparticles (MSNs) have received extensive attention from many researchers for their wide applications in drugs delivery, cell imaging, and catalysis. To date, many delicate intelligent switches have been designed by us and other researchers to control the release of encapsulated cargoes.[4] The mechanisms of these release systems were nearly all based on responsive physical blockage of nanopores in the MSNs, for instance, polymers or nanoplugs (cyclodextrins, nanoparticles, DNA, etc.) leaving the surface of the MSNs. However, although the ability to control and fine tune the release of MSNs had been modestly successful, most of the release systems with blocking units could cause a series of side effects in cells.[4b] Furthermore, the nanopores of most such systems would always be in the "open" state after the blocking units escaping from the nanopores. Thus, these release systems would continue to release the drugs when they escaped from the cells, which would lead to undesirable physiological toxicity and a waste of drugs.[5] Recently, we designed a light-responsive free-blockage release system by controlling the wetting behavior of the surface of MSNs.[4a] However, poor dispersion was a big problem in the biological application of this system. To explore a novel free-blockage release system with good dispersion and biocompatibility that can be controlled along with the change of environment is still a challenging task.

In this paper, we report the design of a pH-responsive free-blockage controlled release system with good dispersion and biocompatibility based on hydrophobic nanopores (Scheme 1). The phenylamine (Ph) group, which has a convertible hydrophobic/hydrophilic property between deprotonation and protonation, was only attached onto the internal surface of the nanopores on the MSNs.[6] The Ph-functionalized nanopores were hydrophobic enough to prevent water entering into the nanopores and so to trap the cargoes in the MSNs at pH 7.0. Meanwhile, the modified MSNs could still be dispersed well in water. With a decrease of the pH value of the solution, the nanopores changed gradually from hydrophobic to hydrophilic, to allow the instrusion of water and release of the cargoes, due to the protonation of the Ph groups. The system also had the ability of sustained release over a long time and could realize pulsatile release with sequential changes between acidic and neutral environments. The pH value of lysosomes is about pH 4.0–5.0, which is lower than the pK_a value of the Ph group ($pK_a \approx 5$), and the pH value of extracellular fluid is nearly neutral, so this novel release system could release antitumor

[a] *Dr. W. Wang, Prof. L.-p. Xu, Prof. H. Du, Prof. Y. Wen, Prof. X. Zhang*
Research Centre for Bioengineering and Sensing Technology
School of Chemistry and Biological Engineering
University of Science and Technology Beijing
Beijing 100083 (P. R. China)
E-mail: wyq_wen@iccas.ac.cn
zhangxueji@ustb.edu.cn

[b] *Dr. L. Chen, Prof. Y. Song*
Key Laboratory of Green Printing, Key Lab of Organic Solids
Beijing National Laboratory for Molecular Sciences (BNLMS)
Institute of Chemistry, Chinese Academy of Sciences
Beijing 100190 (P. R. China)

Supporting information for this article is available on the WWW under http://dx.doi.org/10.1002/chem.201405222.

agents to induce cell death after infecting tumor cells. It could also be transported from the dead cells potentially along with exocytosis from the live cells and further infect the neighboring cells. This effect would greatly improve the drug-transfer efficiency and limit the side effects of undesirable release after the drug carriers escaped from the cells. We believe that this strategy would provide more opportunities for such intelligent free-blockage drug-delivery systems to be used for more practical cancer therapy in the future.

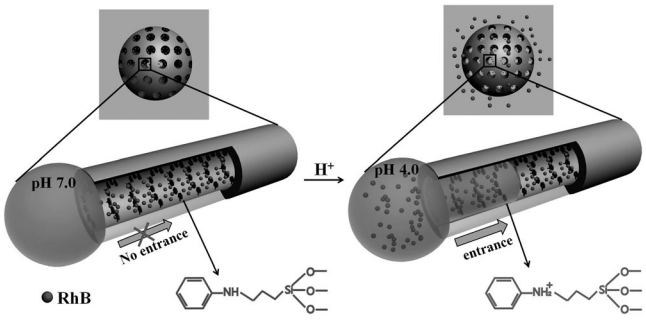

Scheme 1. The release process of the pH-responsive free-blockage controlled release system based on MSNs. This system can release Rhodamine B in acidic conditions.

Results and Discussion

In our research, different concentrations of *N*-phenylaminopropyltrimethoxysilane (PhAPTMS) were chosen to functionalize the internal surface of nanopores on the MSNs by the method of cocondensation under basic conditions (Figure S1 in the Supporting Information). Under the conditions of a constant concentration of surfactant (*N*-cetyltrimethylammonium bromide, CTAB), the molar ratio of PhAPTMS to tetraethylorthosilicate (TEOS) was chosen as 1:10, 1:15, 1:20, or 1:25, and the modified MSNs were accordingly named as MS-Ph (1:10), MS-Ph (1:15), MS-Ph (1:20), and MS-Ph (1:25). As reported in the literature, when the cocondensing reagent contained nonpolar groups, the nonpolar groups tended to intercalate their hydrophobic group into the CTAB micelles to stabilize the formation of cylindrical micelles. After removal of the CTAB micelles, the internal surface of the nanopores functionalized with hydrophobic groups could be made.[6] The UV/Vis absorption peak at around 250 nm gradually increased along with the increase of the ratio (Figure 1).

In the FTIR spectrum of MS-Ph, the absorption peak at 1484 cm^{-1} was attributed to the vibrations of the amino group, and the absorption peaks at 2966 and 2855 cm^{-1} were produced by the vibration of the methylene groups (Figure S11 in the Supporting Information). The thermogravimetric data showed that the weight loss of the four kinds of MS-Ph was increased with the promotion of the modified proportion of the Ph group (Figure S12 in the Supporting Information). These results indicated that the different kinds of MS-Ph were successfully prepared. With MS-Ph (1:20) as an example, the diameter of MS-Ph (1:20) was about 300 nm, the mesoporous channel

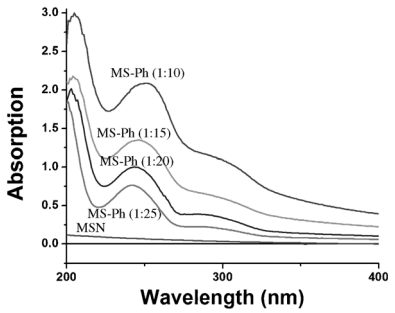

Figure 1. The UV/Vis absorption spectra of the aqueous solutions of differently modified MS-Ph samples (100 $\mu g\,mL^{-1}$; control: water).

could be clearly observed by transmission electron microscopy, the nanoparticles showed typical XRD patterns of MCM-41 type hexagonal mesoporous silica with a lattice spacing of about 4.2 nm, and the N_2 sorption analysis exhibited a type IV isotherm with a total surface area (Brunauer–Emmett–Teller, BET) of 1092.92 $m^2 g^{-1}$ and an average pore diameter of 3.4 nm (Figure 2). The zeta potential of MS-Ph (1:20) was 21.6 mV and the average size of MS-Ph (1:20) was 307.9 nm in aqueous solution, as measured with dynamic light scattering (Figure S8 in the Supporting Information), which was consistent with the diameter of MS-Ph (1:20) in the SEM. (The characterizations of the other three types of MS-Ph are shown in the Supporting Information.)

Rhodamine B (RhB) was chosen as the model cargo. It was loaded into the MS-Ph by dipping the MS-Ph in a solution of toluene/ethanol (4:1) containing RhB. The loading content of RhB was calculated by fluorescence spectroscopy. Fluorescence detection was employed to monitor the release process at 575 nm. With MS-Ph (1:20) as an example, the Ph-modified nanopores appeared to be always physically open, with a diameter of about 3.4 nm (Figure 2), leaving enough space for RhB (1.59 nm × 1.18 nm × 0.56 nm) to exit. However, there is hardly any RhB (approximately 0.43% in 12 h) released from MS-Ph (1:20) at pH 7.0 (Figure 3). This was completely different from the release behavior of the unmodified MSNs at pH 7.0, from which a mass of RhB was released (Figure S13 in the Supporting Information). We speculated that the hydrophobic effect caused by the Ph groups may be the key factor of the controllable loading and release of cargoes. As the pH value of the solution decreased to about 5.0, the RhB was beginning to be released from the MS-Ph (1:20) because of the protonation of the Ph groups, and the release gradually sped up as the pH value was further reduced. Additionally, the rate of release could be decreased with the increased modification ratio of Ph under the same conditions (Figures S14 and S15 in the Supporting Information). When the modification ratio of Ph was decreased to 1:25, release of RhB was observed at pH 7.0 (Figure S16 in the Supporting Information). Moreover, the amount of RhB released from the unmodified MSNs could reach up to 54.7% in 4 h at pH 7.0 (Figure S13 in the Supporting Information), whereas the release percentage of RhB from MS-Ph (1:20) was about 30.9% at pH 3.0 and 22.6% at pH 4.0 in 12 h (Figure 3). These results further demonstrated that this system

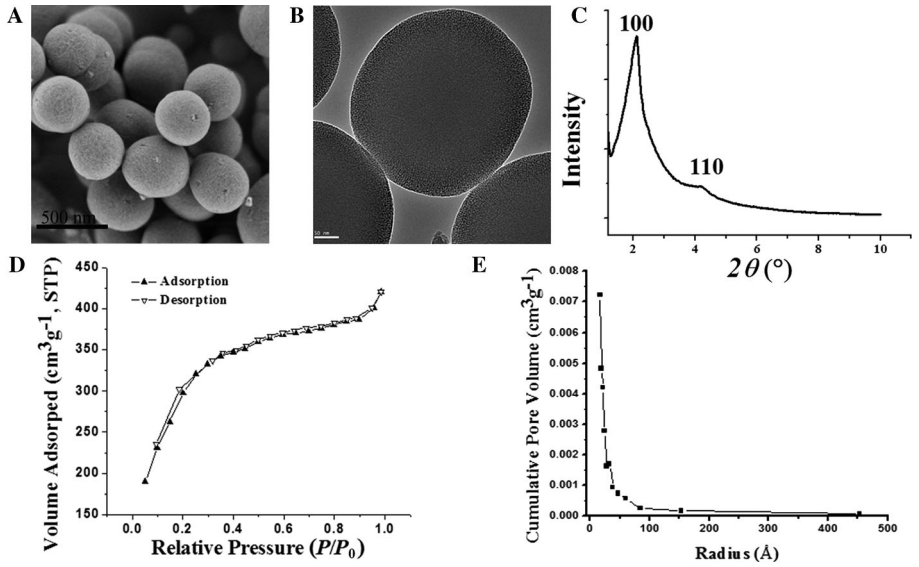

Figure 2. A) SEM image: the average diameter of MS-Ph (1:20) was around 300 nm. B) TEM image: the mesoporous channel could be clearly observed by transmission electron microscopy; scale bar: 50 nm. C) XRD results: a lattice spacing of approximately 4.2 nm was observed. D) N_2 sorption isotherm of MS-Ph (1:20). E) The distribution of pore size of MS-Ph (1:20).

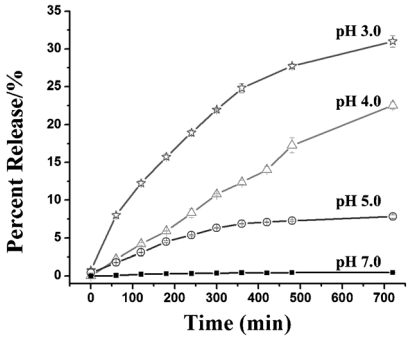

Figure 3. pH dependence of the release profiles of RhB-loaded MS-Ph (1:20). The release gradually sped up as the pH value was reduced.

had the ability for a prolonged duration of drug effect due to the slow release rate caused by the hydrophobic inner surface. This property is particularly beneficial for practical antitumor therapy.[7]

Hydrophobic pores with a small diameter remain dry in water and can withstand a high pressure difference, ΔP, defined by the Laplace equation [Eq. (1)], in which D_{pore} is the pore diameter.

$$\Delta P > 4|\Delta\gamma|/D_{pore} = 4|\gamma\cos\theta|/D_{pore} \quad (1)$$

The difference of surface energy, $\Delta\gamma$, between the solid/vapor surface tension, γ_{sv}, and the solid/liquid surface tension, γ_{sl}, can be related to the contact angle on a flat surface, θ, and the surface tension of the liquid/vapor interface, γ, through the Young equation [Eq. (2)].

$$\Delta\gamma = \gamma_{sv} - \gamma_{sl} = \gamma\cos\theta \quad (2)$$

Therefore, the hydrophobic nanopores could bear a pressure of more than 3.76×10^5 Pa (standard atmospheric pressure: 1.013×10^5 Pa) even for very modest contact angles ($\theta\approx91^\circ$) in quite small pores with $D_{pore}\approx3.4$ nm, which could creat an effective free-blockage "gate" against water intrusion. However, when the contact angle becomes smaller than 90°, this "gate" disappears and opens to the water.

A Ph-modified silica film was used to further prove the convertible hydrophilic/hydrophobic property induced by Ph group. The film would remain hydrophilic due to the low density of the modified Ph group, and it would become hydrophobic when the density of the modified Ph group was increased. MS-Ph (1:25) couldn't keep the RhB in the nanopores, which could be attributed to the low-modification ratio of Ph in the nanopores that cannot hold the water. In addition, the contact angle of the modified films became smaller with a decrease in the modification density of the Ph group and pH value (Figure 4; video in the Supporting Information). These phenomena were consistent with the change in the release rate, which also became much faster with the decrease in the density of the modified Ph group and pH value.

To check the release of RhB from MS-Ph (1:20) under the changeable pH value, we first demonstrated that RhB was released from the container at pH 4.0. The MS-Ph (1:20) was then exposed to a solution of pH 7.0, and a much slower release rate was observed immediately. Importantly, the RhB release profile of MS-Ph (1:20) further presented a pulsatile pattern

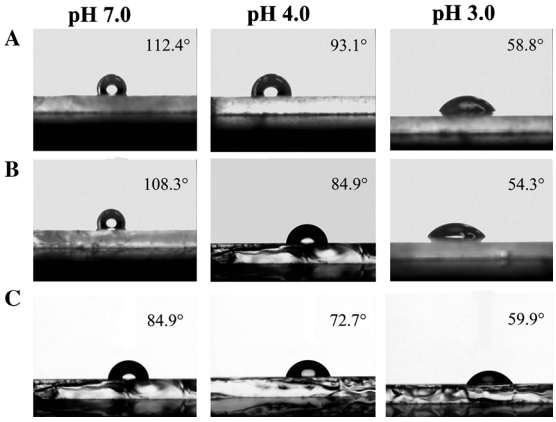

Figure 4. Variation of the contact angle, θ, of the different kinds of silica films at different pH values. A) film 1; B) film 2; C) film 3.

under changing pH values between 4.0 and 7.0 for several cycles (Figure 5). (The data for MS-Ph (1:10) and MS-Ph (1:15) are shown in Figure S17 in the Supporting Information.) The slow water intrusion could be proposed to be a critical factor for the pulsatile release of RhB. In this system, even the acid solution could not wet the whole nanopore in several hours. The inner area of the nanopores would still be hydrophobic and would stop the water going deeper into the nanopores when the MS-Ph was exposed to the neutral solution again. Thus, the pulsatile release was realized with the pH changes over a long period of time. This reversible controllable switch could have more significant application in the complicated physiological environment.

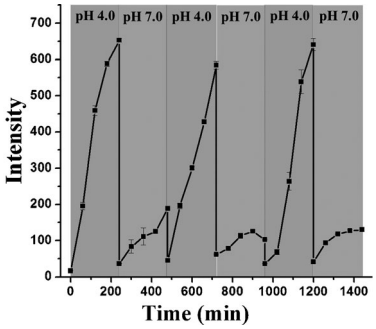

Figure 5. The pulsatile release profiles of RhB-loaded MS-Ph (1:20). The release rate of RhB was changed by sequential adjustment of the pH value of the solution.

Tests of cell viability were further carried out to evaluate the drug-delivery efficiency of this release system on the HeLa cell line. To afford a better release and therapy effect for tumor cells, MS-Ph (1:20) was chosen to deliver antitumor drugs into the cell. In our experiment, epirubicin (EPB), which is a chemotherapy antitumor agent, was loaded into MS-Ph (1:20) to deliver and release the antitumor drug into the tumor cells. The release of EPB was investigated in the same way as that of RhB. The amount of released EPB from the pores of MS-Ph (1:20) was monitored by the change in the fluorescence intensity at 590 nm. As shown in the Figure 6A, the release of EPB gradually sped up as the pH value was reduced, which was the same result as with the release profiles of RhB-loaded MS-Ph. The release percentage of EPB from MS-Ph (1:20) was about 45.1% at pH 4.0 and 12.3% at pH 5.0 in 24 h.

In addition, MS-Ph (1:20) and EPB-loaded MS-Ph (1:20) with different concentrations were separately incubated with the HeLa cells. After 24 h, the cell viability was determined by the standard 3-(4,5-dimethyl-2-thiazolyl)-2,5-diphenyl-2*H*-tetrazolium bromide (MTT) assay. MS-Ph (1:20) exhibited little cytotoxicity even at a concentration of 100 μg mL^{-1} (Figure S18 in the Supporting Information). However, when HeLa cells were coincubated with the EPB-loaded MS-Ph, an obvious reduction of cell viability (≈42.21%) was observed when the concentration of MS-Ph (1:20) was increased to 100 μg mL^{-1}, which was attributed to the release of EPB into the HeLa cells. In addition, the effective endocytosis of MS-Ph (1:20) by HeLa cells was

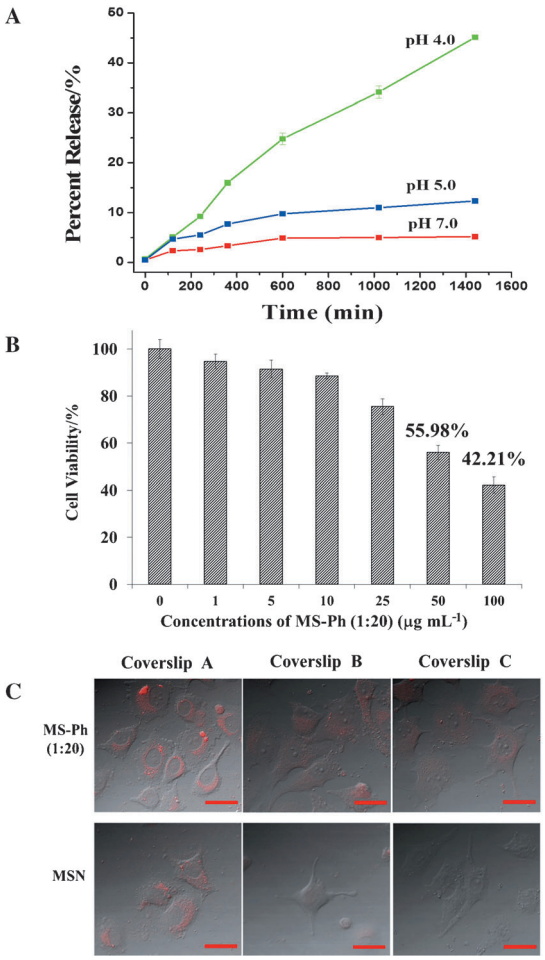

Figure 6. A) pH dependence of the release profiles of EPB-loaded MS-Ph (1:20). The release gradually sped up as the pH value was reduced. B) HeLa cell viability after separate incubation with different concentrations of EPB-loaded MS-Ph (1:20) for 24 h ($P < 0.01$). C) Migration of EPB-loaded MS-Ph (1:20) from the infected HeLa cells to the untreated cells with visualization by using CLSM. The EPB-loaded MSNs (bottom) were observed as the reference. Scale bars: 10 μm.

confirmed by confocal laser scanning microscopy (CLSM; Figure 6C).

To explore the intercellular delivery of EPB-loaded MS-Ph (1:20), HeLa cells seeded on coverslip A were preincubated with EPB-loaded MS-Ph (1:20) for 8 h and then coincubated with fresh cells on the neighboring coverslip B for 20 h. The infection procedure was repeated by coincubating the treated cells on coverslip B with fresh cells on coverslip C for another 20 h. This was followed by observation by using CLSM. As shown in Figure 6C, the red EPB fluorescence in the first treated cells (coverslip A) indicated that EPB was widely distributed in the cells. Additionally, EPB fluorescence was still observed in the infected cells (coverslips B and C). As a control, HeLa cells were treated with the EPB-loaded MSNs. The EPB would be continually released from the unmodified MSNs and scattered in the cell culture when they escaped from the cells (coverslip A). Therefore, unmodified MSNs hardly attained any EPB fluorescence in the infected cells (coverslips B and C). This result proved that this novel release system had the ability to repeat-

edly infect neighboring cells to induce cell death due to the properties of pulsatile release with the sequential adjustment of the pH value.[8]

Similarly, it was proved that the MS-Ph (1:10) and MS-Ph (1:15) could also continuously infect tumor cells. These three types of MS-Ph (1:10, 1:15, and1:20) were all able to realize the intercellular delivery and repeatedly infect the neighboring cells to induce cell death. However, because the release rate became much faster with the decrease in the Ph functionalization, the effect of the drug delivery and therapy would be enhanced (Figures S20 and S21 in the Supporting Information).

Conclusions

In summary, a pH-responsive free-blockage release system was achieved through the conversion of hydrophobic/hydrophilic internal surfaces of nanopores. Cargoes could be trapped in the nanopores in neutral environments due to the hydrophobic effect. In acidic solution, the nanopores were changed to be hydrophilic, which triggered the release of the cargos due to the protonation of the Ph groups. This system also had the ability to sustain the drug release due to the slow water intrusion, which afforded the prolonged drug duration. Furthermore, this release system could also realize pulsatile release with sequential changes between acidic and neutral environments. These advantages made this novel release system available for use as a drug reservoir that could release the antitumor agents to induce cell death after infecting tumor cells and could further infect the neighboring cells without redundant extracellular drug release after transport from the infected cells over a long time. This release system would greatly improve the transfer efficiency of drugs in tumor tissues and reduce the side effects of the containers. The general strategy would open up new possibilities for constructing more practical drug-delivery and controlled release systems.

Experimental Section

Materials

TEOS (99.9%), CTAB (99%), PhAPTMS, RhB, and MTT (98%) were purchased from Sigma Company. Sodium hydroxide, disodium hydrogen phosphate dodecahydrate, and citric acid were purchased from Sinopharm Chemical Reagent Co. Ltd. EPB was purchased from Pfizer. Rosewell Park Memorial Institute (RPMI) medium, Dulbecco's modified Eagle's medium (DMEM), and fetal bovine serum (FBS) were purchased from Life Technologies. All buffers were prepared with ultra-pure MilliQ water (resistance $> 18\ M\Omega\ cm^{-1}$).

Instruments

SEM was performed with a Hitachi SU-8010 instrument. TEM images were obtained by using a TecnaiG2 F20 electron microscope. XRD patterns were collected by using a Rigaku D/max 2500 instrument equipped with Cu_{Ka} radiation. UV/Vis spectra were collected by using a Shimadzu U-1800 spectrophotometer. The zeta potential and dynamic light scattering measurements were collected on a NANO ZS ZEN3600 apparatus. FTIR spectra were recorded on a Bruker-EQUINOX55 spectrometer. Thermal stability measurements were collected on an HCT-3 instrument (Beijing Hengjiu Instruments) between 100 and 550 °C with a heating rate of 10 °C min^{-1}. All fluorescence spectra were recorded on a Hitachi F-4500 FL spectrophotometer in phosphate-buffered saline (PBS) buffer. N_2 adsorption/desorption isotherms were obtained at 77 K on a Micromeritics ASAP2020 automated sorption analyzer. The BET model was applied to evaluate the specific surface areas. Pore size and pore volume were determined from the adsorption data by the Barrett–Joyner–Halenda method. The CLSM images of cancer cells were performed with an Olympus IX83 instrument.

Syntheses

Different modification proportions of MS-Ph

CTAB (0.5 g) was mixed with water (42 mL), ethanol (18 mL), and a solution of sodium hydroxide (0.6 mL, 2 $mol\,L^{-1}$) under stirring for 30 min. Different molar ratios of PhAPTMS (300.7 μL (1:10), 199.7 μL (1:15), 149.8 μL (1:20), and 119.9 μL (1:25)) to TEOS (2.8 mL) were then mixed, respectively, and once added to the mixture in water/ethanol, were stirred at room temperature for 8 h. The resulting different kinds of MS-Ph were separated by centrifugation, washed several times with water and ethanol, and dried in the vacuum oven (60 °C) overnight. Removal of the template was achieved by solvent extraction: MSNs (1.0 g) were suspended in ethanol (100 mL), and the mixture was heated under reflux for 24 h. The solvent-extracted particles were washed extensively with ethanol and collected through centrifugation.

The RhB loaded in the MS-Ph

All kinds of MS-Ph samples (50 mg) were dispersed respectively by sonication into a mixed solution (toluene/ethanol = 4/1, 4 mL) containing RhB (1 mg) for 4 h. The RhB-loaded samples were then collected by centrifugation, washed with water, and dried at 60 °C under vacuum for 12 h before the investigations of the release behavior. The loading content of MS-Ph was calculated by Equation (3) though recycling of the unloaded RhB. The loading contents of the different kinds of MS-Ph were 5.8 (1:10), 5.9 (1:15), 6.2 (1:20), and 2.4 $\mu g\,mg^{-1}$ (1:25), respectively.

$$\text{Percentage of loading} = \frac{\text{total RhB} - \text{unloaded RhB}}{\text{total RhB}} \qquad (3)$$

Testing the RhB release

The release signal was investigated by monitoring the fluorescence intensity of the release system. The standard curve of RhB was established by fluorescence spectroscopy. RhB-loaded MS-Ph (3 mg) was placed in a bottom corner of a cuvette, and PBS solution (citric acid/disodium hydrogen phosphate) was then carefully added to avoid disturbing the MS-Ph. Under some stimuli, the dyes would be released into the solution. Without stimuli, the RhB would not be released from the MSNs and diffused into the solution. The solution could then be directly monitored by fluorescence spectrophotometry to record the release of RhB. For activation of the MSNs, the pH value of the solution was decreased. The amount of guest molecules released from the pores of the MSNs was monitored by the change of the fluorescence intensity at 575 nm.

The hydrophobic/hydrophilic conversion experiment of Ph groups

The silica film was made though the spin coating of silica gel on a glass and dried in an oven for 4 h at 115 °C. Silanization was performed overnight through dipping these films in different concentrations of PhAPTMS in toluene solution (3, 2, or 1%). Modified films were washed with ethanol and cured for 4 h at 115 °C, and named as film 1, film 2, and film 3, respectively. There are two droplets in the videos in the Supporting Information. The pH value of the left one was consistent with the name of videos; the pH value of the right one was pH 7.0. The hydrophobic/hydrophilic conversion of the Ph groups was proved by the change of the contact angle of the modified films.

The biocompatibility studies of MS-Ph

HeLa cells were plated in 96 wells as cell culture clusters at a density of 1×10^4 cells per well and cultured in 5% CO_2 at 37 °C for 12 h. Different concentrations of MS-Ph (1:20; 100 μL) were then added to the media, and the cells were incubated in 5% CO_2 at 37 °C for 24 h. Cell viability was determined by the standard MTT assay.

Cell experiment

To test the effect of the drug delivery in the cell line, HeLa cells were plated in 96 wells as cell culture clusters at a density of 1×10^4 cells per well and cultured in 5% CO_2 at 37 °C for 12 h. The antitumor agent EPB was loaded into MS-Ph (1:20); the EPB loading content of MS-Ph (1:20) was 6.74 μg mg^{-1}. EPB-loaded MS-Ph (1:20; 100 μL) samples with different loading concentrations (1, 5, 10, 25, 50, and 100 μg mL^{-1}) were separately incubated with the cells for 4 h. The cells were then washed twice with PBS buffer before fresh growth medium was added for further incubation for 24 h. After 24 h of incubation, the cell viability was determined by the standard MTT assay.

To explore the intercellular delivery of EPB-loaded MS-Ph (1:20) to the neighboring cells, HeLa cells seeded on coverslip A at a density of 3×10^3 were preincubated with EPB-loaded MS-Ph (1:20; 100 μg mL^{-1}, 100 μL) for 8 h. Coverslip A was then washed twice with PBS buffer and coincubated with fresh cells with a density of 3×10^3 on the neighboring coverslip B for 20 h. The infection procedure was repeated by coincubating the treated cells on coverslip B with fresh cells on coverslip C with a density of 3×10^3 for another 20 h. This was followed by observation by using CLSM. As a control, EPB-loaded MSNs were tested for the effect of intercellular delivery in the same way as that for EPB-loaded MS-Ph (1:20).

Acknowledgements

The authors would like to thank the NSFC (21171019, 51373023, 21073203, 21275017, 21127007, 21103009), the Beijing Natural Science Foundation (2122038), and the Fundamental Research Funds for the Central Universities and NCET-11-0584.

Keywords: controlled release · drug delivery · hydrophobic/hydrophilic effects · mesoporous materials · silica

[1] a) A. R. Parker, C. R. Lawrence, *Nature* **2001**, *414*, 33–34; b) X. F. Gao, L. Jiang, *Nature* **2004**, *432*, 36–36.

[2] a) J. Lee, T. Laoui, R. Karnik, *Nat. Nanotechnol.* **2014**, *9*, 317–323; b) K. Murata, K. Mitsuoka, T. Hirai, T. Walz, P. Agre, J. B. Heymann, A. Engel, Y. Fujiyoshi, *Nature* **2000**, *407*, 599–605; c) G. Ren, V. S. Reddy, A. Cheng, P. Melnyk, A. K. Mitra, *Proc. Natl. Acad. Sci. USA* **2001**, *98*, 1398–1403.

[3] a) I. Vlassiouk, C. D. Park, S. A. Vail, D. Gust, S. Smirnov, *Nano Lett.* **2006**, *6*, 1013–1017; b) F. Rios, S. Smirnov, *ACS Appl. Mater. Interfaces* **2009**, *1*, 768–774; c) M. R. Powell, L. Cleary, M. Davenport, K. J. Shea, Z. S. Siwy, *Nat. Nanotechnol.* **2011**, *6*, 798–802; d) F. Rios, S. N. Smirnov, *Chem. Mater.* **2011**, *23*, 3601–3605; e) S. N. Smirnov, I. V. Vlassiouk, N. V. Lavrik, *ACS Nano* **2011**, *5*, 7453–7461.

[4] a) L. Chen, W. Wang, B. Su, Y. Wen, C. Li, Y. Zhou, M. Li, X. Shi, H. Du, Y. Song, L. Jiang, *ACS Nano* **2014**, *8*, 744–751; b) H. Yan, C. Teh, S. Sreejith, L. L. Zhu, A. Kwok, W. Q. Fang, X. Ma, K. T. Nguyen, V. Korzh, Y. L. Zhao, *Angew. Chem.* **2012**, *124*, 8498–8502; *Angew. Chem. Int. Ed.* **2012**, *51*, 8373–8377; c) P. H. Zhang, F. F. Cheng, R. Zhou, J. T. Cao, J. J. Li, C. Burda, Q. H. Min, J. J. Zhu, *Angew. Chem.* **2014**, *126*, 2403–2407; *Angew. Chem. Int. Ed.* **2014**, *53*, 2371–2375; d) Z. L. Zhao, H. M. Meng, N. N. Wang, M. J. Donovan, T. Fu, M. X. You, Z. Chen, X. B. Zhang, W. H. Tan, *Angew. Chem.* **2013**, *125*, 7635–7639; *Angew. Chem. Int. Ed.* **2013**, *52*, 7487–7491; e) A. Popat, S. Jambhrunkar, J. Zhang, J. Yang, H. W. Zhang, A. Meka, C. Z. Yu, *Chem. Commun.* **2014**, *50*, 5547–5550; f) Z. Z. Yu, N. Li, P. P. Zheng, W. Pan, B. Tang, *Chem. Commun.* **2014**, *50*, 3494–3497; g) S. V. Bhosale, *Chem. Eur. J.* **2014**, *20*, 5253–5257; h) A. Li, J. Zhang, Y. Xu, J. Liu, S. Feng, *Chem. Eur. J.* **2014**, *20*, 12945–12953; i) X. Ma, Y. Zhao, K. W. Ng, Y. Zhao, *Chem. Eur. J.* **2013**, *19*, 15593–15603; j) C. Théron, A. Gallud, C. Carcel, M. Gary-Bobo, M. Maynadier, M. Garcia, J. Lu, F. Tamanoi, J. I. Zink, M. Wong Chi Man, *Chem. Eur. J.* **2014**, *20*, 9372–9380; k) W. Wang, Y. Wen, L. Xu, H. Du, Y. Zhou, X. Zhang, *Chem. Eur. J.* **2014**, *20*, 7796–7802; l) X. Yang, Z. Liu, Z. Li, F. Pu, J. Ren, X. Qu, *Chem. Eur. J.* **2013**, *19*, 10388–10394; m) M. Frasconi, Z. C. Liu, J. Y. Lei, Y. L. Wu, E. Strekalova, D. Malin, M. W. Ambrogio, X. Q. Chen, Y. Y. Botros, V. L. Cryns, J. P. Sauvage, J. F. Stoddart, *J. Am. Chem. Soc.* **2013**, *135*, 11603–11613; n) T. M. Guardado-Alvarez, L. S. Devi, M. M. Russell, B. J. Schwartz, J. I. Zink, *J. Am. Chem. Soc.* **2013**, *135*, 17652–17652; o) J. Zhang, Z. F. Yuan, Y. Wang, W. H. Chen, G. F. Luo, S. X. Cheng, R. X. Zhuo, X. Z. Zhang, *J. Am. Chem. Soc.* **2013**, *135*, 5068–5073; p) Z. X. Zhang, D. Balogh, F. A. Wang, I. Willner, *J. Am. Chem. Soc.* **2013**, *135*, 1934–1940.

[5] R. E. Yanes, D. Tarn, A. A. Hwang, D. P. Ferris, S. P. Sherman, C. R. Thomas, J. Lu, A. D. Pyle, J. I. Zink, F. Tamanoi, *Small* **2013**, *9*, 697–704.

[6] B. G. Trewyn, I. I. Slowing, S. Giri, H. T. Chen, V. S.-Y. Lin, *Acc. Chem. Res.* **2007**, *40*, 846–853.

[7] a) R. Vivek, R. Thangam, V. NipunBabu, C. Rejeeth, S. Sivasubramanian, P. Gunasekaran, K. Muthuchelian, S. Kannan, *ACS Appl. Mater. Interfaces* **2014**, *6*, 6469–6480; b) J. V. Natarajan, A. Darwitan, V. A. Barathi, M. Ang, H. M. Htoon, F. Boey, K. C. Tam, T. T. Wong, S. S. Venkatraman, *ACS Nano* **2014**, *8*, 419–429; c) Y. L. Cheng, C. L. He, J. X. Ding, C. S. Xiao, X. L. Zhuang, X. S. Chen, *Biomaterials* **2013**, *34*, 10338–10347; d) Y. M. Guo, J. Zhang, L. L. Jiang, X. M. Shi, L. Yang, Q. L. Fang, H. Fang, K. Wang, K. Jiang, *Chem. Commun.* **2012**, *48*, 10636–10638.

[8] C. Y. Ju, R. Mo, J. W. Xue, L. Zhang, Z. K. Zhao, L. J. Xue, Q. N. Ping, C. Zhang, *Angew. Chem.* **2014**, *126*, 6367–6372; *Angew. Chem. Int. Ed.* **2014**, *53*, 6253–6258.

Received: September 11, 2014
Published online on ■■ ■■, 0000

FULL PAPER

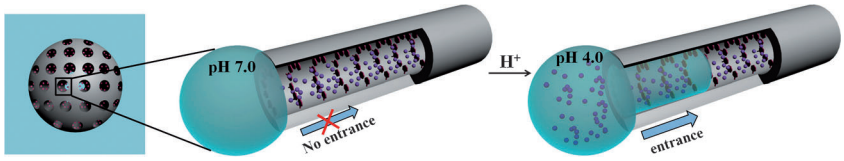

An open and shut case: A pH-responsive free-blockage release system was achieved through controlling the hydrophobic/hydrophilic conversion of mesoporous silica nanopores (see figure). This system could have the ability of continuous infection to tumor cells with high drug-delivery efficiency and few side effects.

Drug Delivery

W. Wang, L. Chen, L.-p. Xu, H. Du, Y. Wen, Y. Song, X. Zhang**

■■ – ■■

A Free-Blockage Controlled Release System Based on the Hydrophobic/Hydrophilic Conversion of Mesoporous Silica Nanopores